

# Fuzzy Control of Humanoid Robot for Obstacle Avoidance

Ching-Chang Wong, Chi-Tai Cheng, Kai-Hsiang Huang, and Yu-Ting Yang

## Abstract

A fuzzy system based on the obtained information of four infrared (IR) sensors and one electronic compass is proposed and implemented on a humanoid robot to avoid obstacles. A humanoid robot named TWNHR-3 with 26 degrees of freedom (DOFs) is designed so that it can do five basic motions. Four IR sensors and one electronic compass are installed on TWNHR-3 to detect the environment information including obstacles, the distances of the obstacles, and the directional angle of the robot. Based on the obtained information, an obstacle avoidance method is proposed to decide one behavior from five motions so that it can avoid obstacles and go to the destination area effectively. Some MATLAB simulation results with different number of obstacles and two real experiments are presented to illustrate the effectiveness of the proposed method.

**Keywords:** Humanoid robot, Biped robot, Autonomous mobile robot, Obstacle avoidance.

## 1. Introduction

For the widely potential use, humanoid robots have been studied for decades by a lot of research groups. Researchers at Waseda University started the humanoid robot research since 1966, and they recently developed a biped humanoid robot WABIAN-2 [1-2]. Honda Corporation developed the humanoid robot Asimo, which has 34 degrees of freedom (DOFs), 120 cm height, and 43 kg weight [3-4]. The Japanese National Institute of Advanced Industrial Science and Technology and Kawada Industries have jointly developed HRP-2 and HRP-2P from 1998. HRP-2 has 30 DOFs, 154 cm height, and 58 kg weight [5-7]. Technical University of Munich developed the humanoid robot JOHNNIE for realization of dynamic 3-D walking and jogging motion. It has 17 DOFs, 180cm height, and 37 kg weight [8]. Sony Corporation also developed several compact size humanoid robots including SDR-3X, SDR-4X, and QRIO. QRIO

has 38 DOFs, 58 cm height, and 7 kg weight [9]. The University of Tokyo developed H6 and H7. The robot has 35 DOFs, 137 cm height, and 55 kg weight [10-11]. Recently, Beijing Institute of Technology has developed a humanoid robot called BHR-02, which has 32 DOFs, 160 cm height, and 63 kg weight [12]. Korea Advanced Institute of Science and Technology developed KHR-3 humanoid (HUBO), which has 41 DOFs, 125 cm height, and 55 kg weight [13]. Team Nimbro from University of Freiburg has developed humanoid robot Paul. The robot has 24 DOFs, 60 cm height, and 2.9 kg weight. The robots with a packet PC as the controller can play soccer [14].

Although the humanoid robot has been investigated for many years, there are still many issues to be studied. There are many studies on obstacle avoidance problem [15-17]. In this paper, we want to solve a real-time obstacle avoidance problem when the robot is navigating in an unknown environment. The picture of the problem is shown as Figure 1. The robot has to start from the center of the start zone to the end zone without obstacle collision. Real-time obstacle avoidance of humanoid robots in dynamic unstructured environments requires processing of large sensory mental tasks without any explicit computations. Humans use perceptions of time, shape, and other attributes of physical and mental objects [18]. In this paper, an obstacle avoidance method based on the fuzzy system concept is proposed and implemented on a compact size humanoid robot named TWNHR-3 to navigate in an unknown environment by using on-line sensory information. Fuzzy logic method is able to represent human expert's knowledge and does not require the mathematical model of the considered system. It is also able to describe the input state continuously. The proposed fuzzy system promises an efficient method for obstacle avoidance.

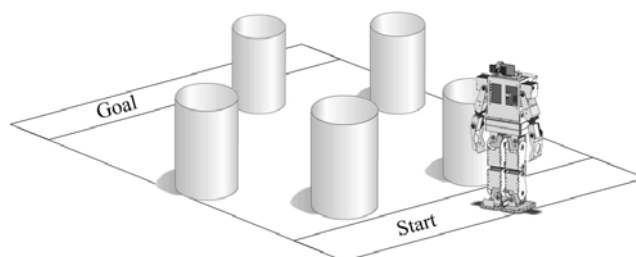


Figure 1. The picture of the obstacle avoidance problem.

Corresponding Author: Ching-Chang Wong is with the Department of Electrical Engineering, Tamkang University, Tamsui, Taipei Hsien, Taiwan.

E-mail: wong@ee.tku.edu.tw

Manuscript received 17 Sep. 2007.

The rest of this paper is organized as follows: In Section 2, the hardware architecture of TWNHR-3 is described. In Section 3, a fuzzy method for obstacle avoidance is proposed. In Section 4, some simulation results and two experiment results are presented to illustrate the effectiveness of the proposed fuzzy obstacle avoidance method. In Section 5, some conclusions are made.

## 2. Hardware Architectures of TWNHR-3

A small-size humanoid robots named TWNHR-3 is implemented and considered in the obstacle collision problem. A vision sensor (a CMOS sensor), four IR sensors, and a direction sensor (an electronic compass) are equipped on the body of TWNHR-3 to obtain the environment information. A control board with a FPGA chip and a 64 M bytes flash memory are mainly utilized to control the robot. Many functions are implemented on this FPGA chip. It can receive the vision signal obtained by the CMOS sensor via a serial port and process the data obtained from the digital compass. It can also process the high level artificial intelligence, such as the navigation. The main design concept of TWNHR-3 is light weight and compact size. The implemented robot TWNHR-3 has 46cm height and 3.1kg weight. The photograph of the established TWNHR-3 is shown in Figure 2. The mechanical design of this robot are shown in Figure 3. The arrangements of hardware architectures for TWNHR-3 are depicted in Figure 4. The details hardware and control software design are described in the following subsections.

### A. Mechanism of TWNHR-3

The mechanical design of TWNHR-3 is described in Figure 3. There are 2 DOFs on the neck, 2 DOFs on the trunk, 8 DOFs on the arm, and 14 DOFs on the two legs. In order to realize the normal walking motion of human, 7 DOFs are adopted to implement the joints of one leg. Owing to the two legs take a great part weight of the whole body, two motors are used in the knee joint design to enforce the robustness of legs. In the neck design of this robot, 2 DOFs is adopted so that the head of the robot can turn right-and-left and up-and-down. The coordinate frame of the legs of TWNHR-3 is shown in Figure 5, where  $l_R$ ,  $l_L$ , and  $\theta$  respectively denote link lengths of right and left legs, and rotation angle of the joint. The motion sequence of one cycle of walking is divided into six phases. Front view, top view, and side view of the six phases are shown in Figure 6. The robot moves the gravity to left leg in first phase. Then the robot raises the right leg and moves forward in the second phase. The robot puts the raising leg down and keeps

balance in the third phase. In the second half cycle, the robot moves the gravity from the left leg to the right leg in the fourth phase. The robot raises the left leg and move forward in the fifth phase. In the sixth phase, the robot puts the raising left leg down and finishes the whole walking cycle. The simulation result of dynamic walking gait for flat ground is shown in Figure 7.

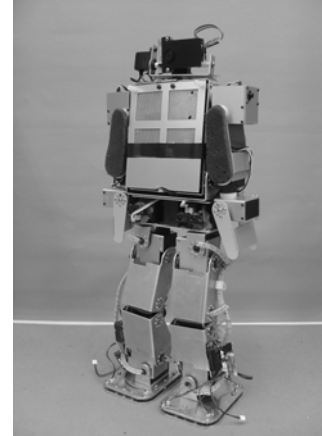


Figure 2. Photograph of the humanoid robot TWNHR-3.

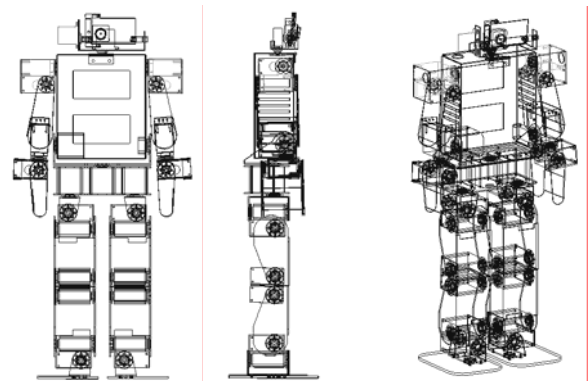


Figure 3. Mechanical design of TWNHR-3.

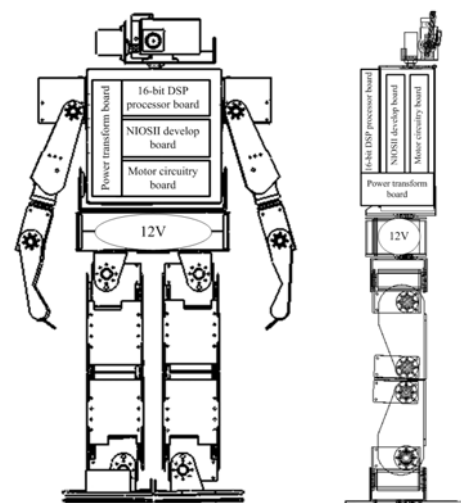


Figure 4. Hardware architectures for TWNHR-3.

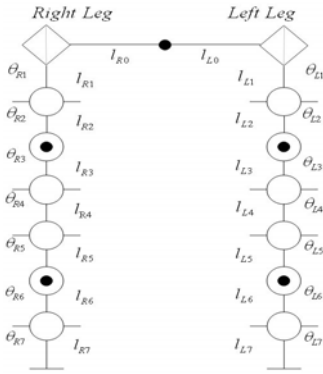


Figure 5. Coordinate frames of legs of TWNHR-3.

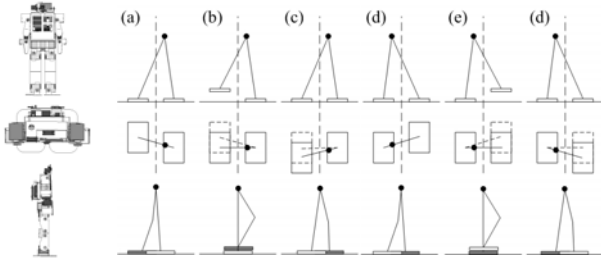


Figure 6. Front view, top view, and side view of the motion sequence of one cycle.

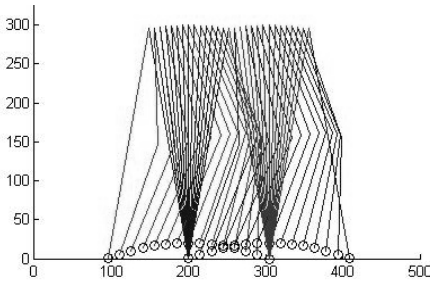


Figure 7. Simulation of walking gait for flat ground.

### B. Processing System

TWNHR-3 consists two micro controllers, a 16-bit DSP ( $\mu$ 'nsp) and a 32-bit NIOS processor. The 16-bit  $\mu$ 'nsp processor obtains the image information from the CMOS sensor. The 32-bit NIOS processor is an embedded soft core processor manufactured by Altera. The system block diagram is described in Figure 8, where 26 servomotors with high torques are used as the actuators of the robot. The term NIOS processor system refers to a NIOS processor core, a set of on-chip peripherals, on chip memory, and interfaces to off-chip memory, all implemented on a single Altera FPGA chip. NIOS processor obtains the environment information from four IR sensors and one electronic compass. It communicates the

computer via RS-232 to transmit and receive the data. The walking motion, which designed from the computer, is stored in the FPGA chip. The  $\mu$ 'nsp processor processes the image information and makes a strategy decision. The NIOS system executes the decision motion from the strategy decision. For the flexible reason, a flash memory is chosen to store the database of the motion of the robot. In this way, the user can adjust the motor angle of robot's motion such as the motion of walk or turn on the PC via the human-machine interface. Then these motion data is saved on the flash memory so that the FPGA chip will read the motion data from the flash memory when the  $\mu$ 'nsp processor decides the robot's motion. Many functions are implemented on a FPGA chip to process the data and control the robot so that the weight of TWNHR-3 is reduced.

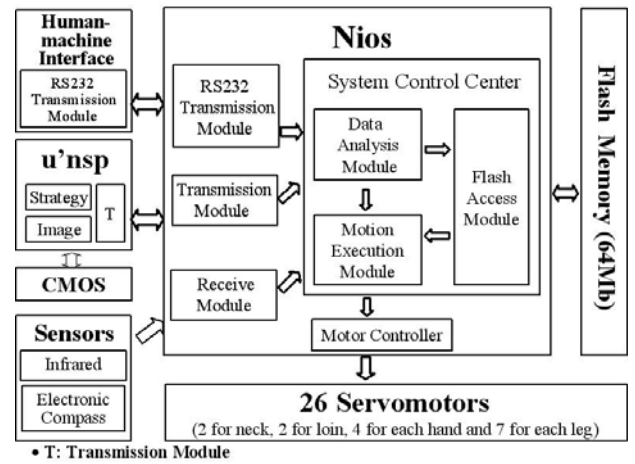


Figure 8. System block diagram of the robot in the electronic system design.

### C. Sensor Module

There are two main parts in the vision module of TWNHR-3: a CMOS sensor and the 16-bit DSP ( $\mu$ 'nsp). The environmental image of the field is captured by the CMOS sensor and the position information of the objects is processed and extracted by the  $\mu$ 'nsp processor. The CMOS sensor is installed in the head of the robot so that the vision of the field can be obtained. The captured image data by the CMOS sensor is transmitted to the  $\mu$ 'nsp processor via a serial port. Based on the given color and size of the object, the  $\mu$ 'nsp processor can process the captured image data to determine the positions of the detected objects in this image. The noise of the environmental image can be eliminated by the  $\mu$ 'nsp processor. An example of color image is shown in Figure 9, where two balls with two different colors are detected in the captured image. After resize the picture and image processing, the cross marks in Figure 9(b)

denote each center of each color region. Based on the extracted position information, an appropriate strategy is made and transmitted to the FPGA chip via a serial transmission.

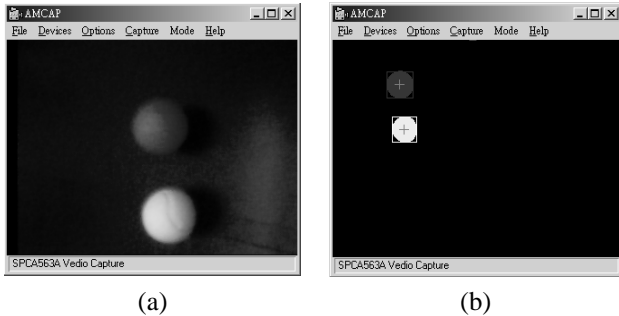


Figure 9. Color detection from the input image. (a) Picture from the original image. (b) Picture after the processing of the image.

Four IR sensors and an electronic compass are mounted on the robot to obtain some environmental information. The maximum detectable distance of the IR sensor is 80cm. The detectable ranges of these four IR sensors are described in Figure 10. One digital compass is installed on the body to detect the head direction of the robot. In order to reduce the weight of robot, the concept of SOC design is applied in the complexity design of humanoid robot. The implemented FPGA chip can process the data obtained from the digital compass and generate desired pulses to control the angles of servomotors.

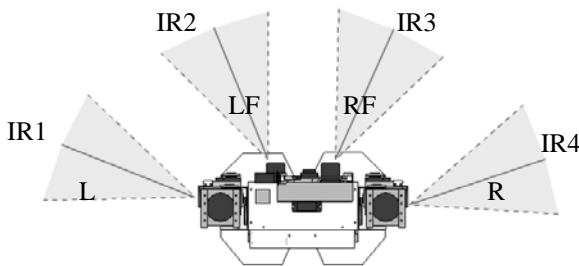


Figure 10. Detectable ranges of four IR sensors.

D. Human-Machine Interface

A human-machine window interface is designed and implemented by BCB to control and monitor the locomotion of the humanoid robot. This human-machine interface is designed to be a convenient development platform to shorten the develop time of the locomotion control design. All of the robot statuses, environment variables, and the learning abilities can be adjusted and analyzed from this interface. Besides, the interface also provides a real-time motion design module. User can see the behavior of robot right away. The window display of this

interface is shown in Figure 11. Five basic motions: (a) Slip Left ( $m_1$ ), (b) Turn Left 30 degrees ( $m_2$ ), (c) Step Forward ( $m_3$ ), (d) Turn Right 30 degrees ( $m_4$ ), and (e) Slip Right ( $m_5$ ) are designed for the robot's movements. The diagram of these five motions is shown in Table 1. In "Slip Left (Right)" motion, the robot can slip toward its left (right) side about 5 cm. In "Turn Left (Right)" motion, the robot first does a 30 degrees left (right) turn then moves forward about 5 cm. The robot will walk forward about 5 cm in "Step Forward" motion.

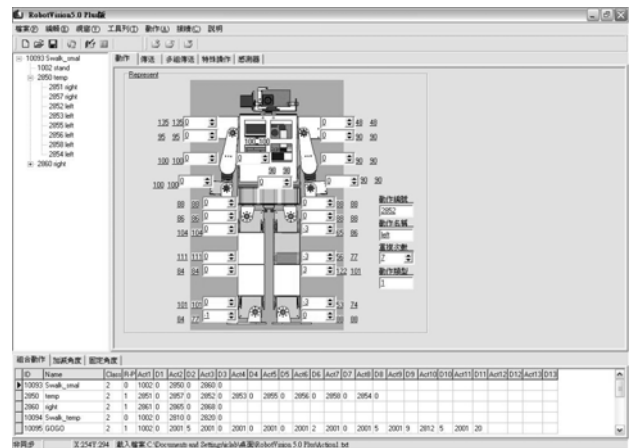


Figure 11. Window display the real-time module of the human-machine interface.

Table 1. The diagram of the five motions.

( $m_1$ )	( $m_2$ )	( $m_3$ )	( $m_4$ )	( $m_5$ )
	30 degrees	Step Forward	30 degrees	

3. Obstacle Avoidance Algorithm

Based on the obtained information from sensors, an obstacle avoidance method is proposed to decide one behavior from five basic motions. In each decision, an appropriate motion  $m_k$  is selected by the following rule:

$$k = \arg \max_{i \in \{1,2,3,4,5\}} f_i, k \in \{1,2,\dots,5\} \quad (1)$$

where  $f_i, i \in \{1,2,3,4,5\}$  is the evaluation value of the  $i$ -th motion and described by

$$f_i = f(d_i, \phi_i), \quad (2)$$

where  $d_i$  and  $\phi_i$  are the distance and angle obtained from the electronic compass and IR sensors for the  $i$ -th motion. A two-input-single-output fuzzy system is proposed based on the obtained information from four IR

sensors and one electronic compass. The fuzzy system is able to determine an evaluation value of each motion to avoid obstacles. Therefore, the robot can choose the motion with the best evaluation value to be the next motion and the system block can be described by Figure 12, where five fuzzy systems are used to evaluate these five basic motions. If more than two motions have the same highest evaluation value, the next motion of the robot is decided by the following priority: Step Forward ( $m_3$ ), Turn Left 30 degrees ( $m_2$ ), Turn Right 30 degrees ( $m_4$ ), Slip Left ( $m_1$ ), and Slip Right ( $m_5$ ).

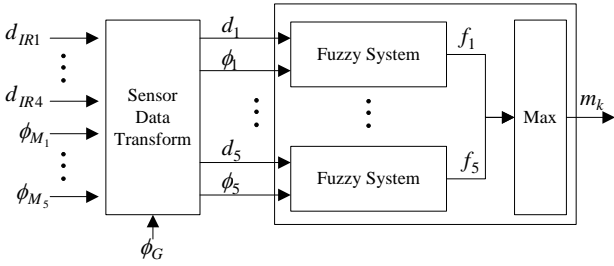


Figure 12. The system diagram of fuzzy controller.

The proposed fuzzy system can be determined by the following five steps:

#### A. Determine input and output variables

As shown in Figure 12,  $d_i$  and  $\phi_i$  are chosen to be the input variables and  $f_i$  are chosen to be the output variable. The input variable  $d_i$  is chosen to be a safety factor of the motion, the input variable  $\phi_i$  is chosen to be a fast factor of the motion, and the output variable  $f_i$  is chosen to be an evaluation value of the motion. Based on the information obtained by IR sensors, the distance  $d_i$  of each motion can be described by

$$d_1 = d_{IR_1} \quad (3)$$

$$d_2 = \min(d_{IR_1}, d_{IR_2}) \quad (4)$$

$$d_3 = \min(d_{IR_2}, d_{IR_3}) \quad (5)$$

$$d_4 = \min(d_{IR_3}, d_{IR_4}) \quad (6)$$

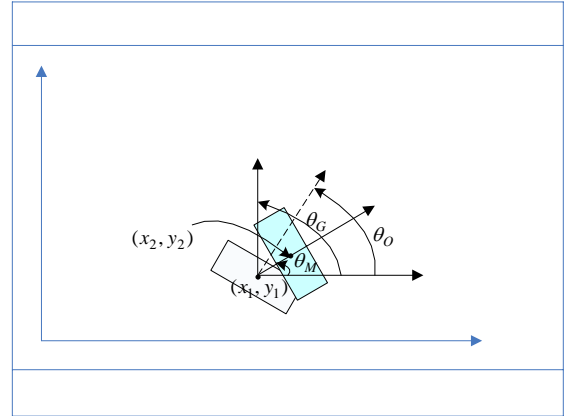
and

$$d_5 = d_{IR_4} \quad (7)$$

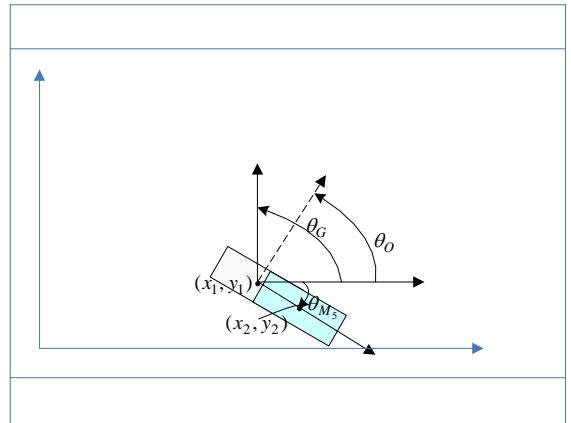
Based on the information obtained by the electronic compass, the angle  $\phi_i$  is the absolute value of the angle difference between the goal direction and the move direction of the  $i$ -th motion and the angle  $\phi_i$  of each motion can be described by

$$\phi_i = |\theta_G - \theta_{M_i}| \quad (8)$$

where  $\theta_G$  and  $\theta_{M_i}$  are the angle of the goal direction and the angle of the move direction when the  $i$ -th motion is executed obtained by the electronic compass. For example, two situations are described by Figure 13, where the robot is at the position  $(x_1, y_1)$  and the original direction  $\theta_0$  of the robot is  $60^\circ$ . If the robot executes the motion  $m_4$  from position  $(x_1, y_1)$  to position  $(x_2, y_2)$ , as shown in Figure 13(a), we can get  $\phi_4 = |\theta_G - \theta_{M_4}| = |90^\circ - 30^\circ| = 60^\circ$ . If the robot executes the motion  $m_5$  from position  $(x_1, y_1)$  to position  $(x_2, y_2)$ , as shown in Figure 13(b), we can get  $\phi_5 = |\theta_G - \theta_{M_5}| = |90^\circ - (-30^\circ)| = 120^\circ$ . The output variable of the fuzzy system is the evaluation value  $f_i$  of the  $i$ -th motion. The more larger the evaluation value of the considered motion, the more suitable to avoid obstacles and the more faster to arrive the goal area of this motion.



(a)



(b)

Figure 13. Description of two situations to determine the input value of  $\phi_i$ : (a) “Right Turn 30 degrees” motion. (b) “Right Slip” motion.

### B. Determine the universe discourses of the input and output variables

The maximal distance detected by the IR sensor is 80 cm. The absolute of the angle difference between the goal direction and the move direction of this new motion is from 0~180 degrees. Therefore, the universe discourses of the input and output variables are selected as  $d_i \in [0,80]$ ,  $\phi_i \in [0,180]$ , and  $f_i \in [0,100]$ .

### C. Determine linguistic values and membership functions

The term sets of the input and output variables are selected as follows:

$$T(d_i) = \{A_1, A_2, A_3\} = \{C, N, F\}, \quad (9)$$

$$T(\phi_i) = \{B_1, B_2, B_3\} = \{S, N, B\}, \quad (10)$$

and

$$T(f_i) = \{C_1, C_2, C_3\} = \{B, N, G\}, \quad (11)$$

where fuzzy sets  $A_1$ ,  $A_2$ , and  $A_3$  are respectively denoted Close (C), Normal (N), and Far (F) for the input variable  $d_i$ . Fuzzy sets  $B_1$ ,  $B_2$ , and  $B_3$  are respectively denoted Small (S), Normal (N), and Big (B) for the input variable  $\phi_i$ . Fuzzy sets  $C_1$ ,  $C_2$ , and  $C_3$  are respectively denoted Bad (B), Normal (N), and Good (G) for the output variable  $f_i$ . The partitions and the shapes of the membership functions are shown in Figure 14, where triangular-type membership functions and fuzzy singleton-type membership function are respectively used for the input and output variables.

### D. Construct a fuzzy rule base

The fuzzy rule base used for the proposed fuzzy system is described in Table 2, where each rule can be described by

Rule  $R(j_1, j_2)$ :

IF  $d_i$  is  $A_{j_1}$  and  $\phi_i$  is  $B_{j_2}$ , then  $f_i$  is  $C_{f(j_1, j_2)}$

$$j_1 \in \{1, 2, 3\}, j_2 \in \{1, 2, 3\}, f(j_1, j_2) \in \{1, 2, 3\} \quad (12)$$

### E. Determine a fuzzy inference method

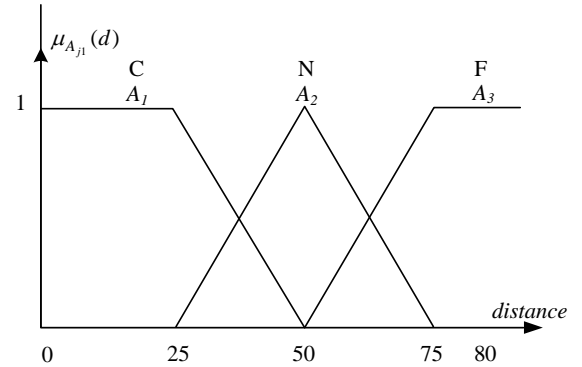
The weighted average method is used to determine the final output of the fuzzy system, it can be described by

$$f_i = f(d_i, \phi_i) = \frac{\sum_{j_1=1}^{j_1=3} \sum_{j_2=1}^{j_2=3} w(j_1, j_2) \cdot v(C_{f(j_1, j_2)})}{\sum_{j_1=1}^{j_1=3} \sum_{j_2=1}^{j_2=3} w(j_1, j_2)} \quad (13)$$

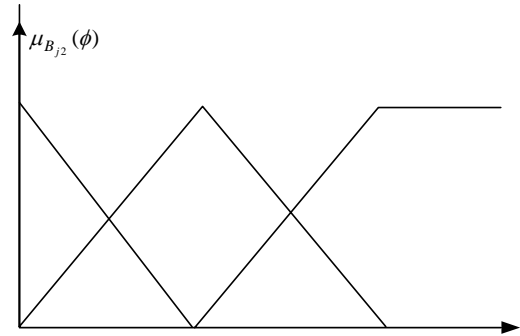
where  $v(C_{f(j_1, j_2)})$  is the crisp value of the fuzzy set  $C_{f(j_1, j_2)}$ .  $w(j_1, j_2)$  is the fire strength of the rule  $R(j_1, j_2)$  and can be described by

$$w(j_1, j_2) = \min(\mu_{A_{j_1}}(d_i), \mu_{B_{j_2}}(\phi_i)) \quad (14)$$

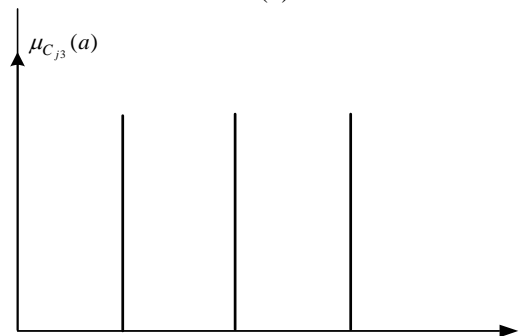
Based on the distance  $d_i$  and angle  $\phi_i$  obtained from the IR sensors and electronic compass for the  $i$ -th motion, five evaluation values  $f_i, i \in \{1, 2, 3, 4, 5\}$  for five basic motions can be determined by these five fuzzy systems. Finally, the proposed method will choose the motion with the best evaluation value to be the next motion of the robot.



(a)



(b)



(c)

Figure 14. Membership functions used in the proposed fuzzy system: (a) Input variable  $d_i$ , (b) input variable  $\phi_i$ , and (c) output variable  $f_i$ .

Table 2. The rule base of the proposed fuzzy system.

$f_i$		$d_i$		
		C	N	F
$\phi_i$	S	B	N	G
	N	B	B	N
	B	B	B	N

#### 4. Simulation and Experiment Results

In order to illustrate the efficiency of the proposed method for the humanoid robot to avoid obstacles. A simulation environment of the obstacle avoidance diagram is constructed and shown in Figure 15, where the scale of the simulation is 5:1. The width of the real robot is 20 cm. The width of the robot in the simulation is 100. There is a finish line marked on one side of the playing field. This side of the playing field is called the finish side. The opposite side of the playing field is called the start side. The two other sides are called side lines. A robot has crossed the finish line when either foot of the robot crosses the finish plane and touches the ground in the end zone. During the competition, the robot does not allow to touch any obstacles.

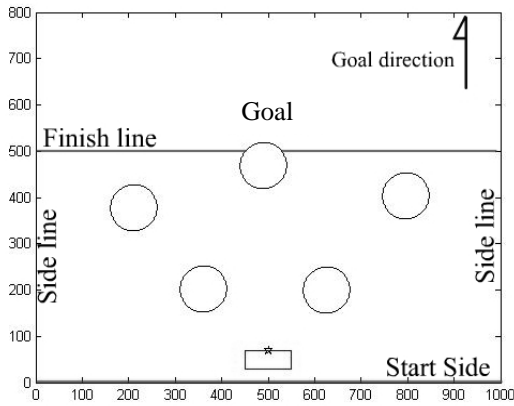


Figure 15. Simulation environment of the obstacle avoidance diagram.

In order to illustrate the proposed method can successfully avoid obstacles and go to the destination, some MATLAB simulations and two real experiments are presented. The whole path of one simulation is shown in Figure 16, where there is one obstacle on the robot's way to the goal line. Six situations in Figure 16 are described in Figure 17 to illustrate the proposed method and their evaluation values of five motions in each situation are described in Table 3. In Situation 1, as shown in Figure 17(a), the robot detects one obstacle which is still far away from the robot and this obstacle reduces down the evaluation value of the motion "Step Forward" to be 80,

but the motion "Step Forward" is the motion with the highest evaluation value. Therefore, the motion "Step Forward" has been chosen as the next motion. In Situation 2, as shown in Figure 17(b), the obstacle is detected by IR2 and IR3 and it is very close to the robot so that the evaluation values of motions "Turn Left 30 degrees", "Step Forward", and "Turn Right 30 degrees" are lower than that in Situation 1. We can see that the evaluation values of motions "Slip Left" and "Slip Right" are the same highest value and the motion "Slip Left" is selected based on the proposed priority. In Situation 3, as shown in Figure 17(c), the obstacle is only detected by IR3 so that the motion "Turn Left 30 degrees" has the best evaluation value (79) and the robot turns left. We can see that the evaluation value of "Step Forward" is raised up to 48 because the robot moves away from the obstacle. In Situation 4, as shown in Figure 17(d), the motion "Step Forward" has the best evaluation value (79) and the robot steps forward. Note that the evaluation value of motion "Slip Right" is zero because the distance  $d_5$  is very small (the robot is very close to the obstacle) and the angle  $\phi_5$  is very big. In Situation 5, as shown in Figure 17(e), the motion "Turn Right 30 degrees" has the best evaluation value (100) and the robot turns right. In Situation 6, as shown in Figure 17(f), the motion "Step Forward" has the best evaluation value (100) and the robot goes toward the goal direction and arrive the goal area (after  $y > 500$ , shown in Figure 15). Furthermore, two environments with two obstacles are considered and described in Figure 18. We can see that the robot will detour round the obstacles, as shown in Figure 18(a) when two obstacles are too close. But the robot will keep going forward, as shown in Figure 18(b) when there is enough space for the robot to walk through. Finally, two environments with three obstacles are considered and described in Figure 19. We can see that the robot is able to choose the suitable motion to avoid obstacles and reach the goal area based on the proposed method.

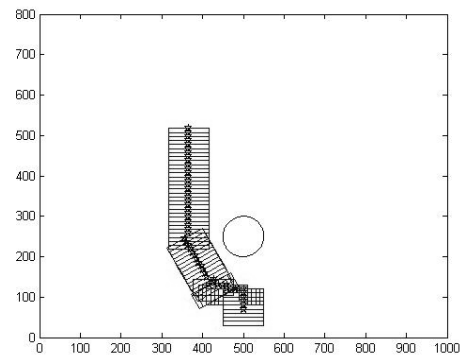


Figure 16. Simulation result of avoiding one obstacle.

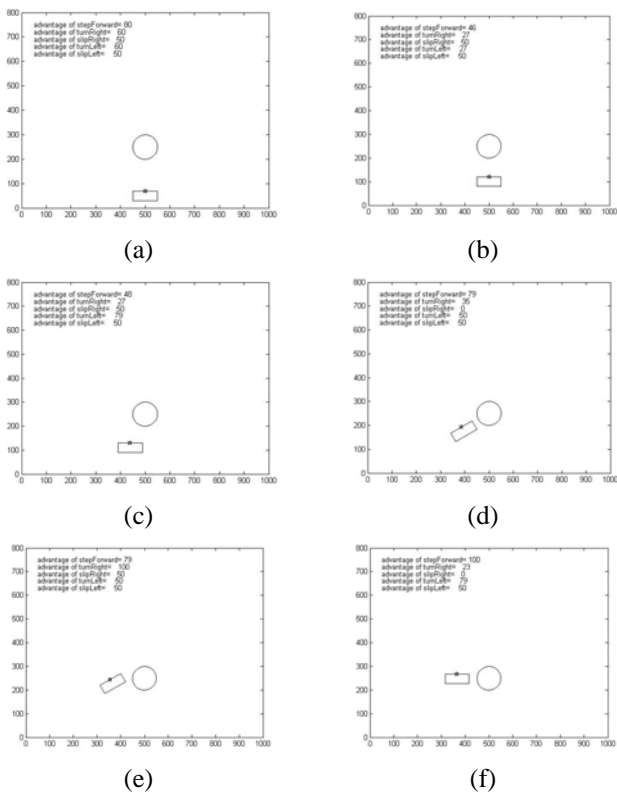


Figure 17. Six situations of the robot for obstacle avoidance described in Figure 16.

Table 3. Evaluation values of five motions for six situations described in Figure 16.

	$f_1$	$f_2$	$f_3$	$f_4$	$f_5$	Selected Motion
Situation 1 (Fig. 16 (a))	50	60	<b>80</b>	60	50	$m_3$
Situation 2 (Fig. 16 (b))	<b>50</b>	27	46	27	<b>50</b>	$m_1$
Situation 3 (Fig. 16 (c))	50	<b>79</b>	48	27	50	$m_2$
Situation 4 (Fig. 16 (d))	50	50	<b>79</b>	35	0	$m_3$
Situation 5 (Fig. 16 (e))	50	50	79	<b>100</b>	50	$m_4$
Situation 6 (Fig. 16 (f))	50	79	<b>100</b>	20	0	$m_3$

In the practical test, the proposed strategy method implemented on TWNHR-3 in a real test ground is discussed. The dimensions of TWNHR-3 are 460 mm in length and 250 mm in width. A real experiment of obstacle avoidance are shown in Figure 20, where one obstacle is set on the robot's way to the goal line. The robot moving toward the goal line is shown in Figure 20(a)-(b). Once TWNHR-3 detects the obstacle via the IR sensors, the robot does an appropriate behavior to avoid obstacles.

The obstacle avoidance motions are shown in Figure 20(c)-(l).

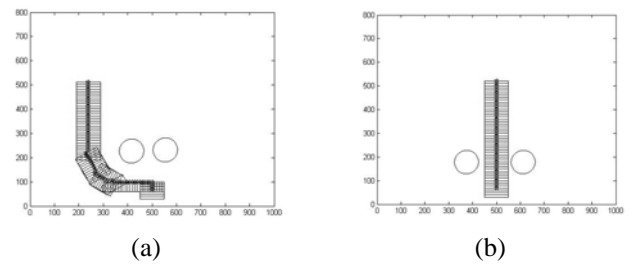


Figure 18. Simulation results of avoiding two obstacles.

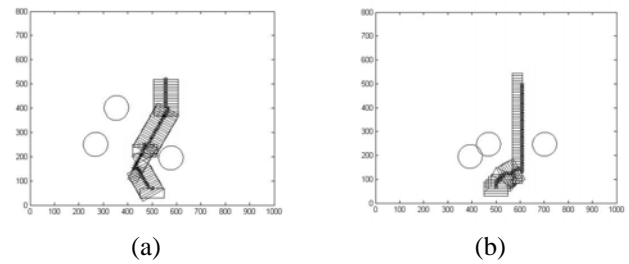


Figure 19. Simulation results of avoiding three obstacles.

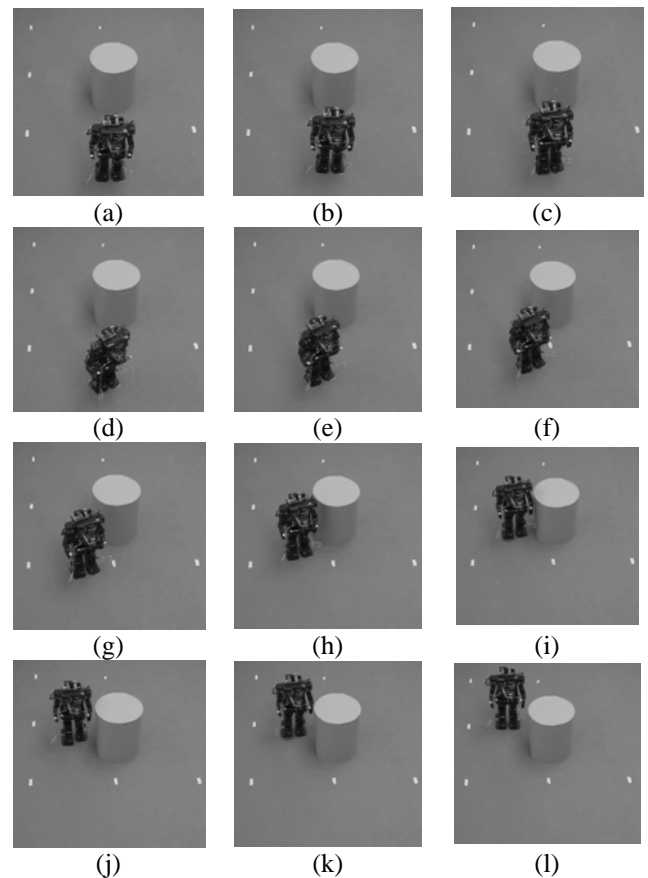


Figure 20. Twelve sequential image stills for a real experiment of the robot to avoid one obstacle by the proposed method.

Moreover, as shown in Figure 21, twelve sequential image stills for a real experiment are presented to illustrate the humanoid robot can avoid three obstacles on the robot's way to a ball (goal) position. First, the pictures of TWNHR-3 avoiding two obstacles and entering the center area are shown in Figure 21(a)-(g). After TWNHR-3 passing through these two obstacles, the pictures of TWNHR-3 detecting the last obstacle and avoiding this obstacle are shown in Figure 21(h)-(l). These two experiment results illustrate that TWNHR-3 can successfully avoid three obstacles and reach the destination area by the proposed strategy method.

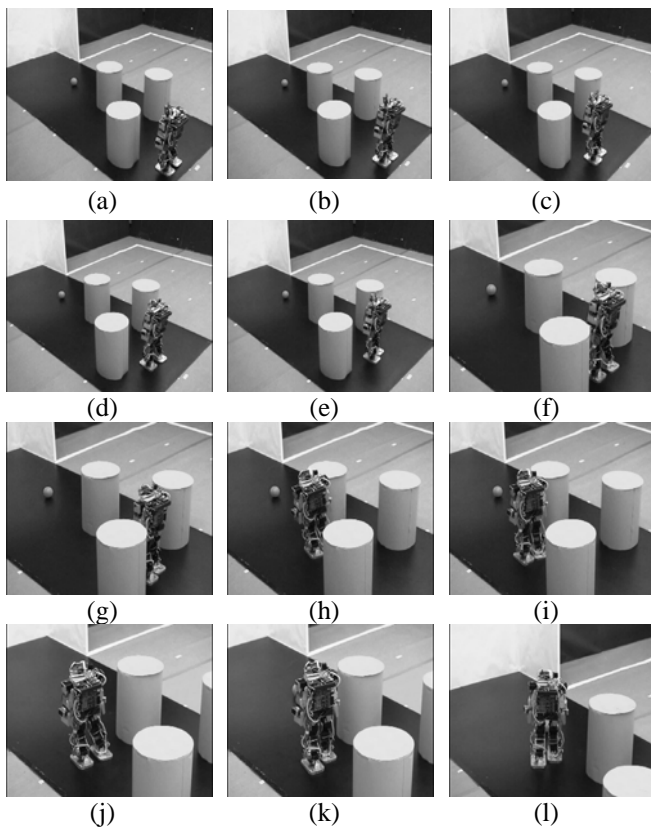


Figure 21. Twelve sequential image stills for a real experiment of the robot to avoid three obstacles by the proposed method.

## 5. Conclusions

An obstacle avoidance method based on the fuzzy system concept is proposed and implemented on the implemented humanoid robot TWNHR-3. Four IR sensors are installed on TWNHR-3 to detect the distance between the obstacles and robot. One electronic compass is set up on TWNHR-3 to get the direction information. Based on the obtained information from these four IR sensors and one electronic compass, the proposed obstacle avoidance method is able to choose a best next motion for the robot. From the simulations and practical experiment results, we can see that the robot can effec-

tively avoid obstacles and successfully arrive the goal line based on the proposed method.

## Acknowledgment

This research was supported in part by the National Science Council (NSC) of the Republic of China under contract NSC 95-2221-E-032-057-MY3.

## References

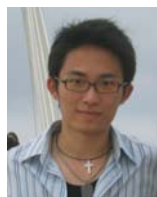
- [1] Y. Ogura, T. Kataoka, H. Aikawa, K. Shimomura, H. Lim, and A. Takanishi, "Evaluation of various walking patterns of biped humanoid robot," *IEEE Int. Conf. on Robotics and Automation*, pp. 605-610, Apr. 2005.
- [2] Y. Ogura, H. Aikawa, K. Shimomura, H. Kondo, A. Morishima, H.O. Lim, and A. Takanishi, "Development of a new humanoid robot WABIAN-2," *IEEE Int. Conf. on Robotics and Automation*, pp. 835-840, Feb. 2006.
- [3] K. Hirai, M. Hirose, Y. Haikawa, and T. Takenaka, "The development of Honda humanoid robot," *IEEE Int. Conf. on Robotics and Automation*, vol. 2, pp. 1321-1326, May 1998.
- [4] Y. Sakagami, R. Watanabe, C. Aoyama, S. Matsunaga, N. Higaki, and K. Fujimura, "The intelligent ASIMO: system overview and integration," *IEEE/RSJ Int. Conf. on Intelligent Robots and Systems*, vol. 3, pp. 2478-2483, Sep. 2002.
- [5] K. Kaneko, F. Kanehiro, S. Kajita, K. Yokoyama, K. Akachi, T. Kawasaki, S. Ota, and T. Isozumi, "Design of prototype humanoid robotics platform for HRP," *IEEE/RSJ Int. Conf. on Intelligent Robots and Systems*, vol. 3, pp. 2431-2436, Sep. 2002.
- [6] K. Fujiwara, F. Kanehiro, S. Kajita, K. Yokoi, H. Saito, K. Kaneko, K. Harada, and H. Hirukawa, "The first human-size humanoid that can fall over safely and stand-up again," *IEEE/RSJ Int. Conf. on Intelligent Robots and Systems*, vol. 2, pp. 1920-1926, 2003.
- [7] K. Kaneko, F. Kanehiro, S. Kajita, H. Hirukawa, T. Kawasaki, M. Hirata, K. Akachi, and T. Isozumi, "Humanoid robot HRP-2," *IEEE Int. Conf. on Robotics and Automation*, vol. 2, pp. 1083-1090, Apr. 2004.
- [8] S. Lohmeier, K. Loffler, M. Gienger, H. Ulbrich, and F. Pfeiffer, "Computer system and control of biped 'Johnnie'," *IEEE Int. Conf. on Robotics and Automation*, vol. 4, pp. 4222-4227, Apr. 2004.
- [9] Y. Kuroki, M. Fujita, T. Ishida, K. Nagasaka, and J. Yamaguchi, "A small biped entertainment robot exploring attractive applications," *IEEE Int. Conf. on*

*Robotics and Automation*, vol. 1, pp. 471-476, Sep. 2003.

- [10] K. Nishiwaki, T. Sugihara, S. Kagami, F. Kanehiro, M. Inaba, and H. Inoue, "Design and development of research platform for perception-action integration in humanoid robot: H6," *IEEE/RSJ Int. Conf. on Intelligent Robots and Systems*, vol. 3, pp. 1559-1564, Oct. 2000.
- [11] K. Nishiwaki, S. Kagami, Y. Kuniyoshi, M. Inaba, and H. Inoue, "Online generation of humanoid walking motion based on a fast generation method of motion pattern that follows desired ZMP," *IEEE/RSJ Int. Conf. on Intelligent Robots and Systems*, vol. 3, pp. 2684-2689, Sep. 2002.
- [12] Q. Huang, Z.Q. Peng, W.M. Zhang, L.G. Zhang, and K. J. Li, "Design of humanoid complicated dynamic motion based on human motion capture," *IEEE/RSJ Int. Conf. Intelligent Robots and Systems*, pp. 3536-3541, Aug. 2005.
- [13] I.W. Park, J.Y. Kim, and J.H. Oh, "Online biped walking pattern generation for humanoid robot KHR-3 (KAIST Humanoid Robot - 3: HUBO)," *IEEE-RAS Int. Conf. on Humanoid Robots*, pp. 398-403, Dec. 2006.
- [14] S. Behnke, M. Schreiber, J. Stückler, R. Renner, and H. Strasdat, "See, walk, and kick: Humanoid robots start to play soccer," *IEEE-RAS Int. Conf. on Humanoid Robots*, pp. 497-503, Dec. 2006.
- [15] H. Seraji, and A. Howard, "Behavior-based robot navigation on challenging terrain: A fuzzy logic approach," *IEEE Trans. Robot. Automat.*, vol. 18, pp. 308-321, Jun. 2002.
- [16] J.H. Lilly, "Evolution of a negative-rule fuzzy obstacle avoidance controller for an autonomous vehicle," *IEEE Tran. Fuzzy Syst.*, vol. 15, pp. 718-728, Aug. 2007.
- [17] Y. Cang, N.H.C. Yung, and W. Danwei, "A fuzzy controller with supervised learning assisted reinforcement learning algorithm for obstacle avoidance," *IEEE Trans. Syst. Man and Cybern.*, vol. 33, no. 1, pp. 17-27, Feb. 2003.
- [18] L.A. Zadeh, "A new direction in AI: Toward a computational theory of perceptions," *AI Mag.*, vol. 22, no. 1, pp. 73-84, 2001.



**Ching-Chang Wong** received a B.S. degree in electronic engineering from Tamkang University, Taipei Hsien, Taiwan, in 1984. He received a M.S. and a Ph.D. degree in electrical engineering from the Tatung Institute of Technology, Taipei, Taiwan, in 1986 and 1989, respectively. He joined the Electrical Engineering Department of Tamkang University in 1989 and now is a professor. His research interests include fuzzy systems, intelligent control, SOPC design, and robot design.



**Chi-Tai Cheng** received a B.S. and a M.S. degree in electrical engineering from Tamkang University, Taiwan, in 2000 and 2002, respectively. She is currently pursuing a Ph.D. degree in electrical engineering from Tamkang University. Her research interests include fuzzy system, robot design and evolutionary algorithms.



**Kai-Hsiang Huang** received a B.S. and a M.S. degree in electrical engineering from Tamkang University, Taiwan, in 2004 and 2006, respectively. He is currently pursuing a Ph.D. degree in electrical engineering from Tamkang University. His research interests include fuzzy system, FPGA design, strategy design, and evolutionary algorithms.



**Yu-Ting Yang** received a B.S. and a M.S. degree in electrical engineering from Tamkang University, Taiwan, in 2005 and 2007, respectively. She is currently pursuing a Ph.D. degree in electrical engineering from Tamkang University. Her research interests include fuzzy system, FPGA design, and evolutionary algorithms.